Science of the Total Environment 536 (2015) 391–405

Contents lists available at ScienceDirect

Science of the Total Environment

journal homepage: www.elsevier.com/locate/scitotenv

Calculating salt loads to Great Salt Lake and the associated uncertainties for water year 2013; updating a 48 year old standard

Christopher L. Shope *, Cory E. Angeroth

U.S. Geological Survey, Utah Water Science Center, 2329 W. Orton Circle, Salt Lake City, UT, 84119, United States

HIGHLIGHTS

- Calculate TDS loads/uncertainties for period of record at inflows to Great Salt Lake
- Comparison of results with previous years to improve estimates of GSL TDS loading
- Seiches limit interpretation of TDS loads under periodic measurement frequencies
- Uncertainty in load estimates is a function of sampling frequency.

GRAPHICAL ABSTRACT

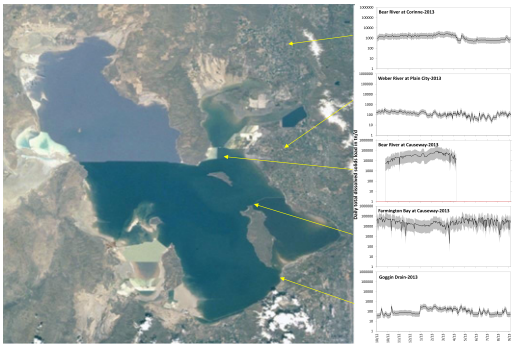

ARTICLE INFO

Article history:
Received 12 May 2015
Received in revised form 4 July 2015
Accepted 4 July 2015
Available online 28 July 2015

Editor: D. Barcelo

Keywords:
Great Salt Lake
Utah
Salt balance
Dissolved solids
Surface discharge
LOADEST
Inland sea/lake
Salinity
Water quality

ABSTRACT

Effective management of surface waters requires a robust understanding of spatiotemporal constituent loadings from upstream sources and the uncertainty associated with these estimates. We compared the total dissolved solids loading into the Great Salt Lake (GSL) for water year 2013 with estimates of previously sampled periods in the early 1960s. We also provide updated results on GSL loading, quantitatively bounded by sampling uncertainties, which are useful for current and future management efforts. Our statistical loading results were more accurate than those from simple regression models. Our results indicate that TDS loading to the GSL in water year 2013 was 14.6 million metric tons with uncertainty ranging from 2.8 to 46.3 million metric tons, which varies greatly from previous regression estimates for water year 1964 of 2.7 million metric tons. Results also indicate that locations with increased sampling frequency are correlated with decreasing confidence intervals. Because time is incorporated into the LOADEST models, discrepancies are largely expected to be a function of temporally lagged salt storage delivery to the GSL associated with terrestrial and in-stream processes. By incorporating temporally variable estimates and statistically derived uncertainty of these estimates, we have provided quantifiable variability in the annual estimates of dissolved solids loading into the GSL. Further, our results support the need for increased monitoring of dissolved solids loading into saline lakes like the GSL by demonstrating the uncertainty associated with different levels of sampling frequency.

Published by Elsevier B.V. This is an open access article under the CC BY-NC-ND license (http://creativecommons.org/licenses/by-nc-nd/4.0/).

1. Introduction

Effective management of surface water resources for human use and ecological health requires unbiased information on the flux of water-quality constituents transported by streams and rivers from upstream

* Corresponding author.
E-mail addresses: cshope@usgs.gov (C.L. Shope), angeroth@usgs.gov (C.E. Angeroth).

http://dx.doi.org/10.1016/j.scitotenv.2015.07.015
0048-9697/Published by Elsevier B.V. This is an open access article under the CC BY-NC-ND license (http://creativecommons.org/licenses/by-nc-nd/4.0/).

landscapes to downstream receiving waters. To better understand the nature of upstream sources of constituent mass and the relative contributions from different source areas, the constituent flux or load must be known or estimated. As climate change continues to impact hydrological and ecological systems, forecasting physical and water quality responses throughout the watershed can greatly improve management decisions (Aherne et al., 2006; Elsdon et al., 2009; Tweed et al., 2011). The effective design and evaluation of water-quality management programs requires both a robust estimate of constituent concentration or load and the uncertainty associated with the estimation of the flux estimates.

Typically the constituent flux is estimated as an average rate of the total mass passing a location over time. Ideally, the flux is quantified by integrating the product of concentration and discharge over regular and frequent time steps throughout a period of interest. Commonly, discharge is estimated by frequent stage measurements calibrated to discharge through the use of a site- and time-specific rating curve (Shope et al., 2013). However, concentration measurements are usually sparsely collected due to the expense of sample analysis and the logistical difficulties. To estimate the temporal flux, available concentration measurements are used to interpolate estimates for periods when no measurements were collected.

Many techniques have been developed to estimate the water-quality flux of specific constituents. Of these, multiple regression analysis of flux based on observed discharge, time, and season are commonly utilized (Cohn et al., 1989, 1992; Crawford, 1991; Dolan et al., 1981; Ferguson, 1986, 1987; Preston et al., 1989; Robertson and Roerish, 1999; Robertson and Saad, 2011; Runkel et al., 2004; Runkel, 2013; Stenback et al., 2011). While simple linear regression of the constituent concentration versus discharge can provide a reasonable estimate to predict concentrations at times that were not sampled, statistical estimation methods typically provide more robust predictive capabilities. An example is the USGS LOADEST (Runkel, 2013; Runkel et al., 2004) software package that analyzes up to 9 specified regression models with the option to create additional user-specified models. LOADEST estimates constituent flux as a function of discharge, time, and season. The model also uses a number of bias diagnostics including summary statistics, the Partial Load Ratio (Stenback et al., 2011), Load Bias, Nash-Sutcliffe Efficiency Index (Nash and Sutcliffe, 1970), and residual outputs. The benefits of more robust statistical flux estimation techniques include assessment of the systematic error associated with bias and the random error associated with variance. Random error is expected and defines the standard error surrounding the flux estimate, although systematic error is more problematic and is introduced by unexpected watershed and in-stream processes. Bias diagnostics with statistical models can be applied to salt load estimates to discern sample collection differences or dynamic processes such as precipitation and wind-driven transport.

Continuous salt flux estimates of inputs to the Great Salt Lake (GSL) have generally been nonexistent and to our knowledge, calculation of the estimate uncertainty has not been completed. GSL is a remnant of the prehistoric Lake Bonneville and is the largest hypersaline lake in the Western Hemisphere. It is the fourth-largest terminal lake in the world with salinity ranging from 1.4 to 8.0 times greater than the ocean. Saline lakes account for nearly 45% of the total global inland lake volume (Shiklomanov, 1990) and are therefore an important part of the landscape. The GSL ecosystem annually supports between 2 and 5 million migratory waterfowl and shorebirds from throughout the Western Hemisphere (Aldrich and Paul, 2002) and was designated a part of the Western Hemisphere Shorebird Reserve Network in 1992. The lake supports brine shrimp (*Artemia franciscana*), which are a valuable food supply for migratory birds and the brine shrimp cyst harvest industry with annual revenues as high as $60 million. The maximum adult brine shrimp salinity tolerance is approximately 30%, near the saturation level of 28%. Artemia require salinity less than 10% to initiate hatching but optimal cyst production ranges from 14–17% (Lenz and Browne, 1990; Van Stappen, 2002). The $1.1 billion GSL mineral extraction industry includes at least 4 corporations annually producing 3.2 million metric tons of salts, including NaCl, $MgCl_2$, and K_2SO_4. These industries can have conflicting objectives in terms of managing GSL salinity. For example Gunnison Bay is too saline to provide brine shrimp habitat; however, it provides an adequate pre-concentration step for mineral extraction activities. Because of the importance of the lake to wildlife and industry, an accurate understanding of the spatiotemporal dissolved solid balance within the lake is needed. Previous studies have primarily focused on salt concentration as a function of lake elevation and GSL processing (Mohammed and Tarboton, 2011, 2012). However, to our knowledge only two studies have attempted to quantify salt loading from inflows to the lake (Hahl, 1968; Loving et al., 2000). In fact, the results from Hahl (1968) have been the accepted steady-state input rate of dissolved salts into the GSL.

The objective of this study is to assess the spatiotemporal salt load into GSL for water year 2013 and describe the associated estimate uncertainty. We compare these results to previous estimates for water years 1960, 1961, and 1964, which have formed the basis for mineral extraction volumes since 1968. Even with the long history of scientific investigations, quantification of the spatial distribution and the temporal salt load into GSL remain elusive. For this study, we collected major ion chemistry and surface water discharge measurements at the dominant surface water inflow locations to the GSL to quantify the dissolved salt loading into the GSL for water year 2013. This approach has the benefit of evaluating changes in dissolved salt loading to GSL over time, which is necessary for operational management activities. In addition, the utility of incorporating a multi-variate statistical approach provides uncertainty bounds on observational quality and frequency that is useful to a broad range of surface water investigations.

2. Study location and physiography

The Great Salt Lake (40.7°N–41.7°N, 111.9°W–113.1°W) is in the northeast Great Basin province (Fig. 1). The mean lake elevation, based on 169 years of record, is 1279.8 ± 0.9 AMSL. The GSL drainage areas is about 55,000 km^2 and the lake is the fourth largest, perennial, closed-basin lake in the world (Mohammed and Tarboton, 2011). The Wasatch Mountains are east of the lake and the Oquirrh and Stansbury Mountains lie to the south, while the relatively uninhabited Bonneville Salt Flats lie to the west. GSL development was in response to tectonic extension of the eastern Basin and Range Province in the middle Tertiary (Miller, 1991). Numerous faults trending N–S and NE–SW are situated in the GSL and bioherm structures suggest that the faults served as conduits for sub-lacustrine discharge of groundwater (Colman et al., 2002). Marine sediments from Glacial Lake Bonneville dominate the area, which due to lake recession and evaporative processes, has left large concentrations of dissolved minerals such as potash and halite in the surrounding soils. The GSL watershed was investigated from 1998 to 2001 (Waddell et al., 2004) and results indicated that the majority of streambed sediment concentrations of selected trace elements exceeded aquatic standards in streams draining mine tailings and metal smelters. Jones et al. (2008) provide a thorough description of the complex impacts on solute inputs to the closed basin from the weathering of the Precambrian and Paleozoic mountains to the east and the Tertiary and Quaternary sediments to the west.

The Great Salt Lake is fed by direct precipitation, the Bear, the Weber, and the Provo-Jordan Rivers, several other minor streams, and groundwater seepage. The only outflow for the GSL is evapotranspiration, which depends on meteorological conditions, salinity, and lake surface area/altitude (Mohammed and Tarboton, 2011). The GSL is located on a shallow playa, in which small changes in the water-surface elevation results in large changes in the surface area of the lake. The average lake depth ranges from 4–6 m resulting in a surface area that ranges from 3000–6000 km^2 (Mohammed and Tarboton, 2011). The GSL is predominately fed by surface water inflows into the south arm. Therefore,

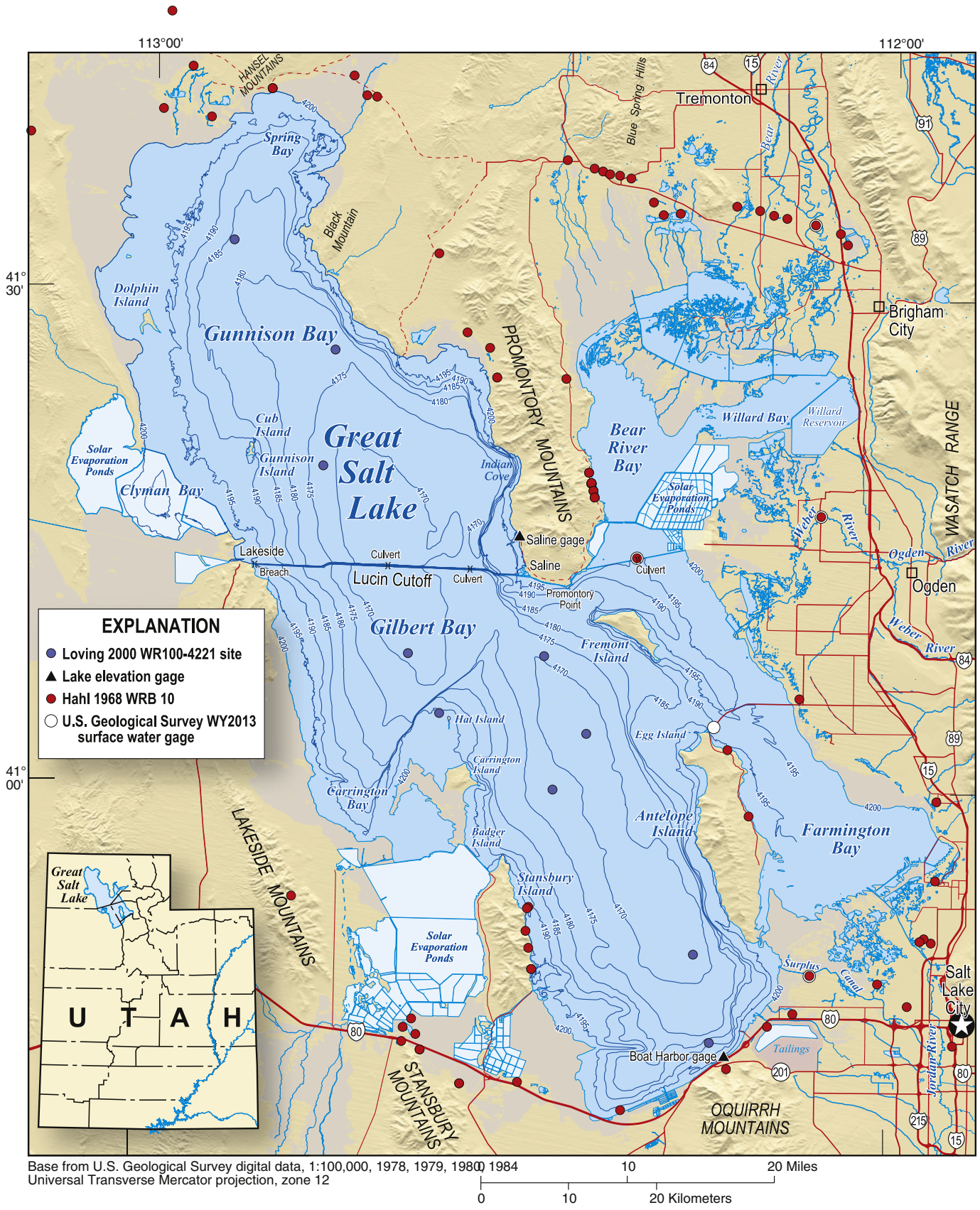

Fig. 1. Great Salt Lake study area location showing monitoring locations used by Hahl, 1968; Loving et al., 2000; and the current study for water year 2013.

the north arm is substantially more saline than the south arm and the lake elevation at the south arm is between 0.06 and 61 m higher than the North arm (Loving et al., 2000). The salinity of GSL ranges between approximately 5% (measured in Gilbert Bay in 1995) to nearly 28% (measured in Gunnison Bay in 1968).

The sampling locations for the Hahl (1968), Loving et al. (2000), and the current study are markedly different although based on similar strategies. Hahl's (1968) objective was to estimate individual dissolved salt loads by surficial sources to GSL in 1960, 1961, and 1964. In 1964, flow was considered average and samples were collected near his defined "lakeshore" boundary. This boundary is a change in topography from sandy beach or boulder-strewn bluffs to flat mud or sandy lakebed. The 1960 and 1961 sample periods were below average flow periods with lower lake elevations and the surface flow of this "lake area" was not contained in defined channels but was affected by wind and brine movement. Hahl (1968) measured or estimated discharge and collected water quality data at 79 locations on tributaries and from springs around the lake. He then used a step-wise time and discharge weighted concentration to presumably estimate the load at each monitoring location. The discreet dissolved solids loads distributed around GSL were aggregated to estimate the total load for water years 1960, 1961, and 1964 from each drainage basin. This approach was labor intensive and dependent on lake elevation. With higher lake elevations, such as water year 2013, many of these seeps and springs may be underwater. In addition, many sampling locations were negligible tributaries. The 21 sampling locations that Loving et al. (2000) used for their study included USGS streamgages distributed throughout the Bear, Weber, and Provo-Jordan River drainages. Our strategy was to aggregate all of the Bear River drainage and Jordan River drainage sampling locations into the discharge entering the GSL at the Bear River and Farmington Bay Causeway monitoring locations, respectively.

Completion of the porous, rock-filled Lucin Cutoff railroad causeway in 1959 divided the lake into a north (Gunnison Bay) arm and south (Gilbert Bay) arm resulting in restricted water and salt exchange between the north and south arms. The exchange of water has been limited to flow through two relatively small culverts and leakage through the porous causeway fill material (Loving et al., 2000). In 1984, the causeway was breached near Lakeside, UT at the western shore of GSL to allow for more rapid flow of water from the south arm to the north arm during high lake elevations. However, due to structural integrity issues, the east and west culverts were closed in 2012 and 2013, respectively, and a new bridge has been proposed to replace the connection between the two arms that the culverts provided.

3. Methods

3.1. Inflow and GSL site locations

The three primary inflows to GSL are the Provo-Jordan River (which separates into the Goggin Drain discharging to Gilbert Bay and the Jordan River discharging to Farmington Bay), the Weber River (discharging to Gilbert Bay near Plain City), and the Bear River (discharging to Gilbert Bay). Four sampling locations account for 93% of the total annual surface water inflow to GSL based on records from 1987 through 1998 (Loving et al., 2000). These locations are Goggin Drain (USGS 10172630 Goggin Drain near Magna UT), Weber River (USGS 10141000 Weber River near Plain City, UT), the Farmington Bay Causeway (USGS 410401112134801 GSL Farmington Bay Outflow at Causeway Bridge), and the Bear River Bay Causeway (USGS 10010060 Bear River Bay Outflow at Causeway Bridge near Warren, UT). In addition, samples were also collected upstream of the Bear River Causeway location at Bear River at Corinne (USGS 10126000 Bear River near Corinne, UT) to facilitate further analysis. The Farmington Bay and Bear River Causeway sites were utilized rather than individual river discharge locations due to logistical and monitoring concerns. The Jordan River diverges many times prior to discharge into Farmington Bay which would require sampling all inflows to Farmington Bay. The Bear River Wildlife Sanctuary lies between the Bear River at Corinne and Bear River Causeway gages, which has significant spatiotemporal evapotranspiration and no flow conditions. Therefore, the Causeway locations were chosen to facilitate direct measurements to Gilbert Bay. Measurements and analysis completed using the Bear River at Corinne gage were for comparative purposes with the Bear River Causeway location; calculated estimates were determined at either of the locations. Between 2 and 4 water quality measurements were completed at these four surface water inflow locations throughout water year 2013 (Fig. 1).

3.2. Field methods

Field parameters including pH, water temperature, and specific conductance (SC) were measured at each of the inflow and lake sites using an In-Situ Troll 9500 multi-parameter water-quality instrument. These measurements were collected opportunistically during water quality sampling at monitoring locations. The total number of in-situ measurements ranged between 5 and 13 for each location during water year 2013. The high-range specific conductance and standard pH probes were calibrated prior to measurements. The temperature probe calibration was verified on an annual basis with a NIST certified thermometer.

Water samples from river inflow sites were analyzed for major ions and total dissolved solids (TDS) by residual on evaporation (ROE) and sum of constituents (SOC). Samples were composited using the equal discharge increment (EDI) method (Wilde et al., 1999) at Bear River Causeway and Farmington Bay Causeway inflow sites and the equal width increment (EWI) method (Wilde et al., 1999) at the Goggin Drain, Weber River, and Bear River near Corinne sites. River inflow samples were composited into a pre-cleaned churn splitter and processed on-site. Water samples were collected from the 5 surface water inflow monitoring locations for major ions, total dissolved solids (TDS), and salinity. A pre-cleaned and dedicated Tygon sampling tube was used at each site to prevent cross-site contamination. Standard USGS protocols were used for water-quality sampling (U.S. Geological Survey, variously dated). Water samples for the analysis of major cations were filtered (Whattman, <0.45 μm) and collected in acid- and field-rinsed, 250 mL polyethylene bottles and acidified to a pH of <2 with 7.7 N Omnitrace nitric acid. Water samples for the analysis of major anions were filtered (<0.45 μm) and collected in field-rinsed 250 mL polyethylene bottles.

3.3. Water quality analysis

Major element concentrations were measured by inductively coupled plasma-atomic emission spectrometry (ICP-AES; Fishman, 1993) at the USGS National Water Quality Laboratory (NWQL), in Lakewood, CO. Major anion concentrations were measured with ion-selective electrode (ISE — Fishman and Friedman, 1989) and ion-exchange chromatography (IC — Fishman and Friedman, 1989) at the USGS NWQL, in Lakewood, CO. Due to the high salinity of the GSL, all samples for major elements were diluted up to approximately 100 times, which has the effect of decreasing the analytical precision for individual analytes. The associated decrease in analytical precision due to sample dilution would therefore propogate to the estimates of the salt loading. However, the decrease in analytical precision is expected to remain negligible relative to the concentrations observed in locations such as the Farmington Bay Causeway.

Samples were analyzed for total dissolved solids (TDS) by residual on evaporation (ROE) and sum of constituents (SOC). Residue on evaporation (ROE) is determined by weighing the dry residue remaining after evaporation of the volatile portion of an aliquot of the water sample; ROE was analyzed for most samples. Additionally, selected samples were analyzed for major ions, and the dissolved-

Table 1
Comparison of model evaluation criteria and bias diagnostics for each of the monitoring locations.

Location	Goggin Drain	Weber River at Plain City	Bear River at Corinne	Farmington Bay Causeway	Bear River Bay Causeway
Site ID	10172630	10141000	10126000	410401112134801	10010060
No. Obs.	44	228	213	21	20
Period of record	11/20/1963–2/24/15	10/1/1959–2/24/2015	10/1/1963–9/20/2000	2/23/2004–2/24/2015	3/12/10–10/25/2013
Model evaluation					
Model selected	3	8	9	9	4
AIC	102.6	−39.96	5.844	56.19	2.2527
SPCC	109.7	−15.9584	32.73	64.54	−24.5185
AICc	103.6	−39.45	6.55	68.19	–
Residual variance	0.5389	0.04746	0.05772	0.5952	0.4537
R-squared	61.42	95.81	88.88	80.78	63.51
P-value	<0.0001	<0.0001	<0.0001	<0.0001	<0.0001
Bias diagnostics					
Bp	−24.19	−0.3981	1.012	−6.348	−5.91
PLR	0.7581	0.996	1.01	0.9365	0.2481
E	0.2105	0.9621	0.926	0.6567	0.2708

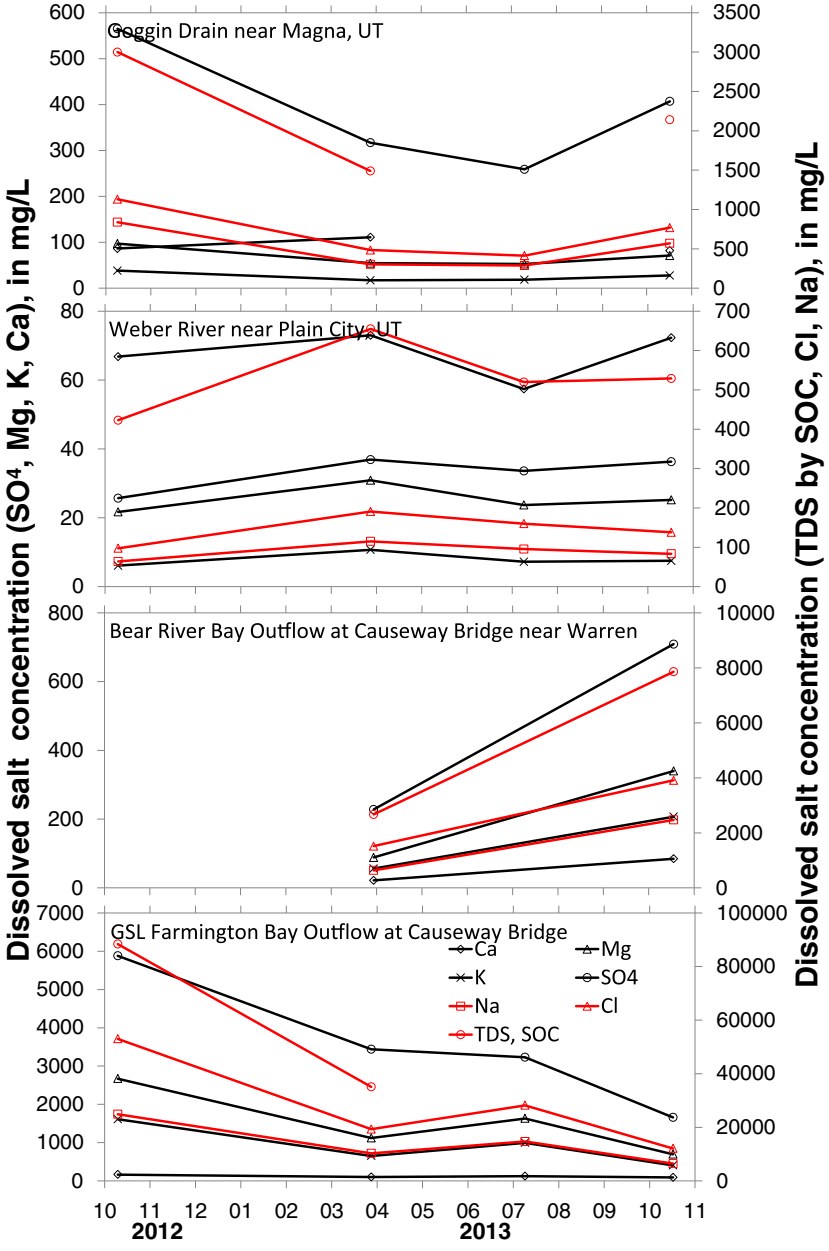

Fig. 2. Major ion and TDS concentrations measured over water year 2013 at Great Salt Lake inflow sites.

solids concentrations of these samples were calculated by the SOC. TDS samples collected throughout this study and those of Hahl (1968) and Loving et al. (2000) included analyses for both ROE and SOC. Our approach was to build a regression of TDS as a function of SC, since TDS and SC are highly correlated. We used the TDS to SC relationship over the entire period of record at each site location to provide a comprehensive assessment of temporal measured and regressed TDS. The period of record for each of the locations is as follows: Goggin Drain (20 Nov 1963–1 Oct 2013), Weber River (1 Oct 1959–1 Oct 2013), Bear River at Corinne (1 Oct 1963–20 Sep 2000), Farmington Bay Causeway (23 Feb 2004–1 Oct 2013), and the Bear River Causeway (12 Mar 2010–1 Oct 2013). Periods when both TDS (ROE) and TDS (SOC) were collected indicated less than 2% difference between method on average. In addition, our approach to populate TDS concentration as a function of SC utilized a mix of both methods when observed TDS concentrations were not available. Therefore, regardless of method of determination, further references will be simply referred to as TDS.

3.4. LOADEST model construction

LOADEST (Runkel, 2013; Runkel et al., 2004) was used to estimate the mass loading of dissolved salinity from each of the surface water inflows into the Great Salt Lake over the entire period of record. The entire period of record was chosen because the low number of TDS observations and regressed TDS estimates for water year 2013 limited the statistical efficacy. Wind driven flow reversals of water discharge from GSL into the Bear River and Farmington Bays were removed from the dataset prior to analysis. Discrete values of TDS from each of the surface water inflow sites were related to daily discharge, time, and up to 7 additional variables that describe annual seasonality and variability in stream discharge of varying length. The variability of stream discharge is further represented using flow anomalies as described by Ryberg and Vecchia (2012).

Nine different models for each inflow site (Runkel et al., 2004; Ryberg and Vecchia, 2012) was examined and the best model was automatically selected and evaluated through model regression statistics

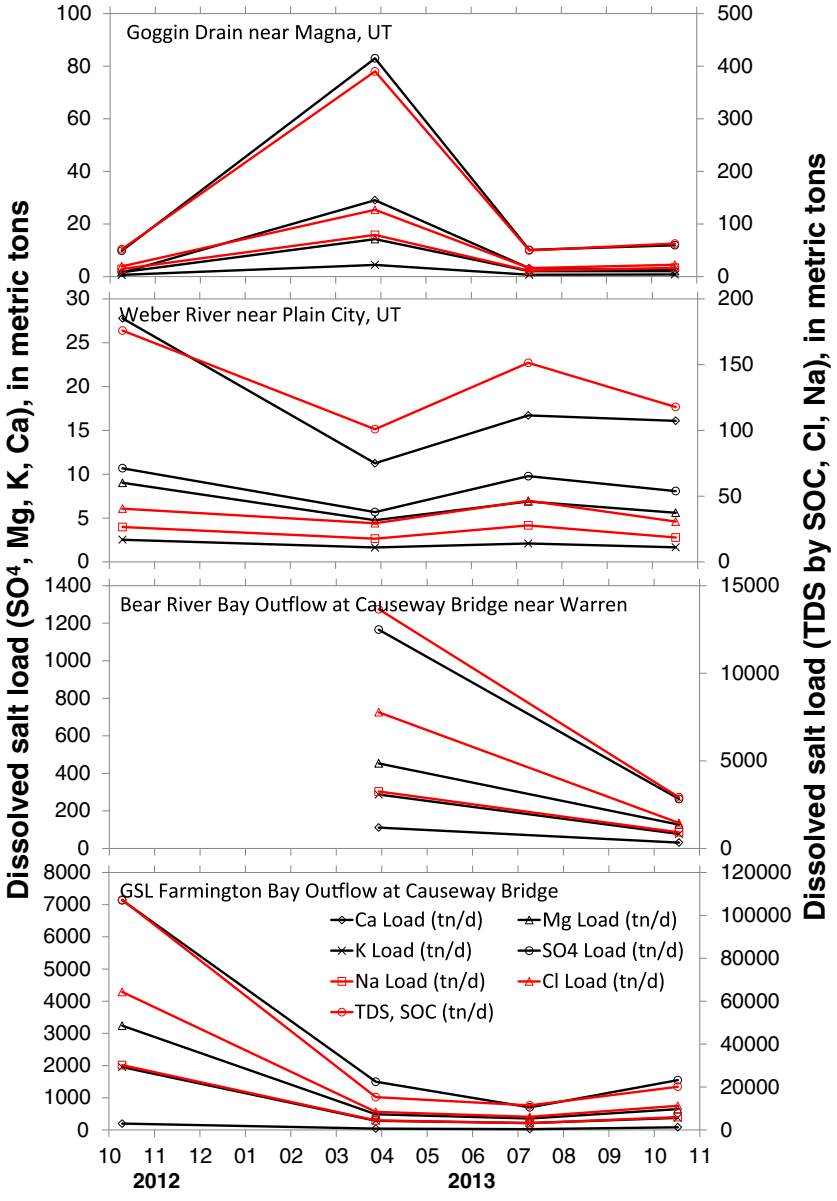

Fig. 3. Major ion and TDS loadings measured over water year 2013 at Great Salt Lake inflow sites.

and bias indicators, diagnostic plots of residuals and fitted values, and Akaike Information Criteria corrected for finite sample sizes (AIC_c) (Akaike, 1973, 1974; Hurvich and Tsai, 1989). The model regression diagnostic statistics included the adjusted R^2 and *p*-values of the variable coefficients. Under the automated selection option, adjusted maximum likelihood estimation (AMLE — Cohn, 1988, 2005) is used to estimate model coefficients for loading values. The diagnostic plots included fitted versus observed values, normal probability plots of model residuals, and model residuals versus the fitted values, discharge, and time. Daily TDS loads were then computed using the best model identified for each site. A summary of the model evaluation criteria and bias diagnostics is provided in Table 1.

In addition to the model form, regression-based estimates of TDS loads are heavily influenced by the sampling frequency and the distribution of samples with respect to season and discharge (Guo et al., 2002; Preston et al., 1989). Since the major ion and TDS samples at each of the inflow sites was collected between 2 and 4 times throughout water year 2013, we were not able to temporally re-sample the values to construct alternative regressions. However, to attempt to characterize temporal sampling bias and error in the regression-based estimates of TDS, we used an alternative location (USGS 09180500 Colorado River near Cisco, UT) with continuous discharge and SC measurements throughout water year 2013. While a monitoring location with continuous SC in the watershed would have been more suitable for similar hydrologic conditions, we feel that the Colorado River at Cisco location provides the data to adequately describe the resampling experiment. The regression of TDS to SC was constructed, similar to that of Shope and Gerner (2014) to calculate the TDS load over time. While 15-minute continuous estimates of TDS loading were used as the observational load estimates, the data were resampled on an hourly, bi-daily, daily, weekly, bi-weekly, and monthly interval. This exercise enabled a quantitative estimate of information loss and increased uncertainty for water year 2013 at this gage site.

4. Results

4.1. Simple regression-based TDS load estimation into GSL

4.1.1. GSL inflow salt load estimation for WY 2013

Measured dissolved salt concentrations in water year 2013 from the Farmington Bay Causeway and to a lesser degree, the Bear River Causeway, were more than an order of magnitude higher than the Weber River and Goggin Drain inflow concentrations. Generally, lower concentrations of all major ions were measured in April and July, which is consistent with flushing of accumulated surficial salt storage during spring runoff, and increased concentrations in late summer and fall (Fig. 2).

The dissolved solids load or flux into the GSL is a more useful measure of the impact the dissolved solids on GSL. The product of the measured concentration of individual major ions from water year 2013 sampling efforts and the average daily discharge were used to compute the dissolved solids load from each of the inflow monitoring locations to the GSL (Fig. 3). As expected, dissolved solids loads increased throughout spring runoff, as evidenced during the April sample collection, and then decreased into the fall. The exception is the Farmington Bay samples where substantially higher discharge and constituent concentrations were observed in October 2012, which elevated the fall 2012 salt load into GSL. The elevated discharge during the October 2012 period relative to the other locations, suggests that wind driven seiches potentially accounted for the abnormally high dissolved solids load at this site. Wind-driven seiches are prevalent on GSL during the fall, causing flow reversals which force saline water into the bays, such as Farmington Bay. As the surface water discharge in Farmington Bay continues, normal flow directionality into GSL from Farmington Bay is resumed but with elevated dissolved salt concentrations. However, with limited sampling frequency, a precise estimate of the retention time of the wind-driven saline GSL contribution in Farmington Bay is not readily apparent.

4.1.2. TDS to SC linear regression

The voracity of temporal loading trends at each of the inflow monitoring locations to GSL may be questionable considering that only between 2 to 4 TDS samples were collected during water year 2013. To bolster our predictive TDS analysis, we regressed TDS as a function of SC during water year 2013, resulting in up to 13 regressed values. We further used the entire period of record at each monitoring location to build a regression of TDS to SC for both TDS measured by sum of constituents (SOC) and residue on evaporation (ROE). SC was then used as a proxy for TDS with a predictive algorithm based on the regression. Since there were more SC measurements than TDS, we developed the algorithm to populate TDS for all measured SC in order to increase the temporal resolution and predictive power. We prescribed a site specific TDS value for every sample where SC was measured; 1) using the TDS by ROE measure if available, 2) using the TDS by SOC measure if available, and 3) using the TDS by ROE regression. The regressed TDS concentration as a function of SC is presented in Fig. 4 for each of the surface water inflows into the GSL. We found that TDS measured by ROE was more accurate as measured by an increase in the coefficient of determination; however, TDS by SOC were more abundant. The slight difference in accuracy can be explained by the error propagation associated with TDS by SOC. For the SOC methodology, the anion and major element constituents have the potential to undergo significant dilution (i.e. selected samples from Farmington Bay inflow), each with an associated error that is summed when the TDS is obtained. In contrast, the TDS by ROE methodology does not have this error propagation. The period of record ranged from 2010 to 2013 at the Bear River Causeway to a period from 1960 to 2013 at the Weber River. This resulted in between 21 (Bear River Causeway) and 479 (Weber River) measured or regressed TDS values (ROE or SOC) for the period of record at each location that ultimately provided stronger model predictive capability. Therefore, with reasonable estimates of TDS concentration over time, we attempted to correlate TDS to average daily discharge observations in order to calculate the daily dissolved solids loading into the GSL.

4.1.3. TDS to discharge linear regression

We compared the estimated TDS concentrations relative to discharge for the entire period of record at each inflow site (Fig. 5). Overall, the regression of TDS to discharge was good at the Bear River at Corinne

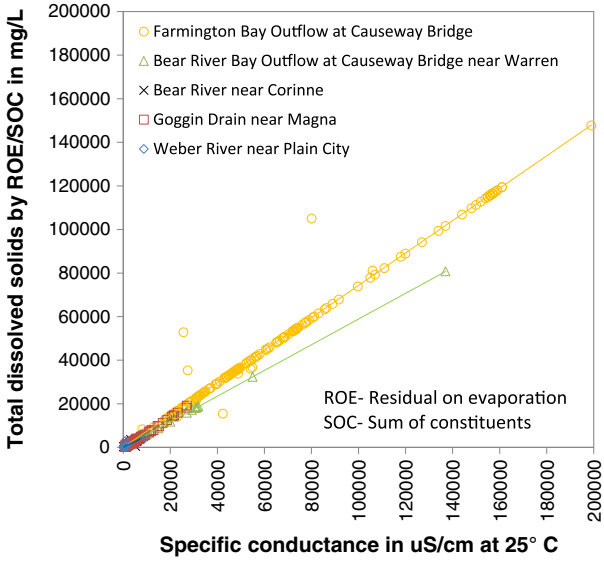

Fig. 4. Regression of site specific TDS to SC for each of the inflow monitoring locations to the Great Salt Lake over the period of record.

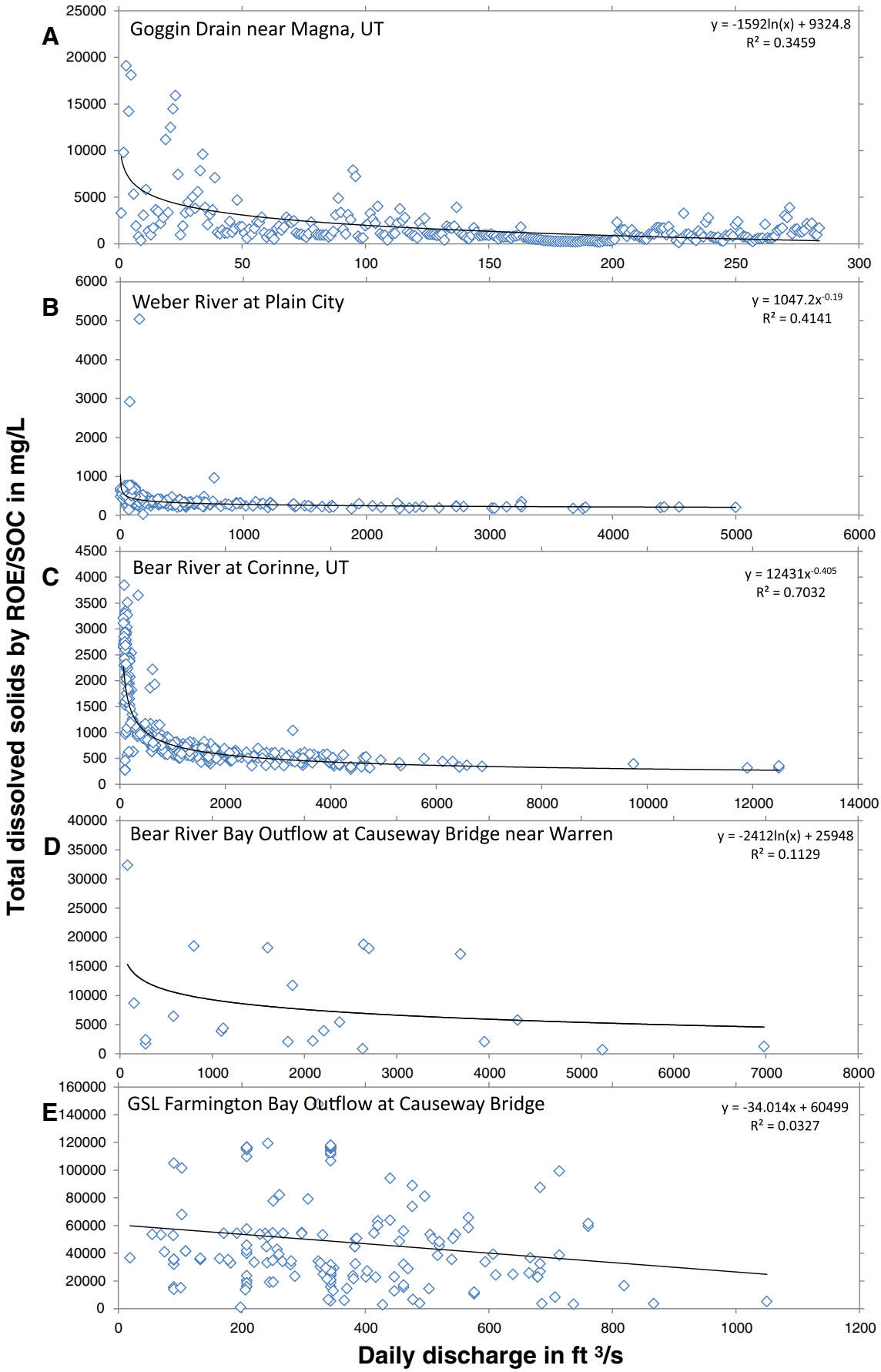

Fig. 5. Regression of TDS concentration to discharge for each of the inflow monitoring locations to the Great Salt Lake over the period of record.

site and reasonable and fairly consistent for the Goggin Drain, Weber River, and Bear River at Corinne locations. However, the regressions for the Bear River and Farmington Bay Causeway monitoring locations were highly variable and showed limited correlation (Fig. 5). During several sampling periods over the entire period of record, reverse or negative discharge was noted at the causeway locations, indicating that flow was from the GSL into the bay. However, these reverse flow incidents were removed from the analysis prior to development of the regressions. There was a higher sample population for the Goggin Drain, Weber River, and Bear River at Corinne sites than the causeway locations, indicating that sample density is an important factor in accurately predicting TDS concentration relative to discharge. Therefore, our results indicate that overall the TDS concentration is not solely explained by discharge over the entire period of record, which increases the uncertainty of the predictive capability of individual measurements.

Since the predictive power of the TDS to discharge relationship was limited over the period of record, we further analyzed the individual inflow monitoring sites for TDS versus discharge on an annual basis (SI 1). Overall, we found a generally better correlation, although with significant uncertainty between individual years. However, for consistency between methods previously applied by Hahl (1968) and Loving et al. (2000), we calculated the TDS loading for water year 2013 at each of the surface water inflow monitoring locations (Table 1).

It remains whether we can better predict TDS concentration as a function of only discharge on an annual basis or over the entire period of record. Our results indicate that annual regressions of TDS to discharge were improved relative to the aggregated result obtained over the entire period of record. However, the R^2 values for individual years varied (SI 1), and in some cases, the relationship was not consistent with the typical trend of decreasing TDS associated with increasing discharge. In addition, many years were not adequately sampled to better inform our estimates of TDS from discharge and therefore, iterating the process over time was not a reasonable means to estimate total dissolved solids loading into GSL.

4.1.4. Annually regressed TDS load estimates for water year 2013

Even with the deviation in linearly regressed model fit between TDS and discharge as identified by R^2 (SI 1), we calculated the daily TDS load from inflows into the GSL for consistency with previously published reports (Fig. 6). We used the initial linear regressions of TDS to discharge over the period of record to estimate the daily TDS load into GSL for water year 2013. The total annual TDS load was further summarized for each of the monitoring locations.

The Bear River at Corinne monitoring location maintained the highest load of the monitored inflows with an average of 2023 metric tn/d. Spring runoff and upstream irrigation withdrawals initiated in May decreased the load five-fold for the remainder of the water year to an average of 399 metric tn/d. The inflows to Farmington Bay were cumulatively measured at the Farmington Bay Causeway monitoring location and displayed the second highest loading to GSL with a relatively constant TDS load of 1089 ± 103 metric tn/d. The TDS load estimated at the Bear River Causeway monitoring location were more stable than the Corinne location and substantially diminished due to the lower discharge. The average TDS loading for the Bear River Causeway monitoring location was 304 ± 26 metric tn/d. The Goggin Drain monitoring location indicated an average load of 103 metric tn/d prior to January 2013. Ice cover prohibited monitoring throughout most of January and by February the TDS load had increased and remained high with an average daily load of 327 metric tn/d. The TDS load from the Weber River monitoring location was typically the lowest at 85 ± 37 metric tn/d and showed significant variability.

Interestingly, the results using this method indicate that the overall TDS load into GSL is approximately 711,000 tons for water year 2013, which is substantially less than the previously estimated (Hahl, 1968) amount of 3,200,000 metric tons. The estimated annual TDS load from the Bear River Causeway was approximately 123,000 tons, while the upstream location of Bear River at Corrine was estimated at 456,000 metric tons for water year 2013. The idea of roughly three times more salt loading at the Corrine gage than the Causeway location entering the GSL seems implausible for several important reasons. Salt loads would be expected to increase with distance downstream and evapotranspiration in Bear River Bay would significantly impact salt loading measured at the Bear River Causeway. In addition, we verified from our linear regressions that many locations had significant uncertainty in the relationship solely based on TDS and discharge and that this uncertainty varied from year to year. These deviations would therefore influence the total load estimates. It is important to note differences in methodology; Hahl (1968) used an annual time and discharge weighted average to calculate the salt loads for each monitoring location. We believe that this estimate can be bolstered by explicitly accounting for temporally variable discharge and TDS as a function of SC for loading estimates. In addition, using the methodology of Hahl (1968), there is not an appealing way to bound these TDS load estimates with confidence intervals or some other measure of variance. Therefore, we used the LOADEST statistical estimator to better calculate continuous loads, the standard error, and the 95% confidence intervals to bound our estimates.

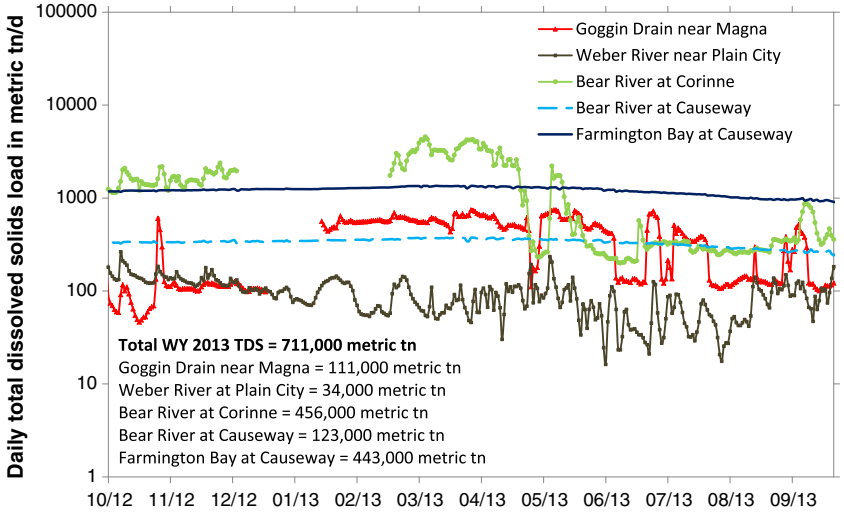

Fig. 6. Daily TDS load estimated from regression to discharge for each of the surface water inflow monitoring locations to the GSL.

Table 2
Comparison of regressed TDS as a function of discharge to statistically derived TDS load estimates for each of the inflow monitoring locations to GSL in water years 1960, 1961, 1964, and 2013.

	Sample year	Monitoring location	Regressed	Mean daily	LOADEST TDS load			Hahl (1968)	Mean daily
			TDS load	Streamflow	Average	Low 95% CI	High 95% CI	TDS load	Streamflow
			(Metric tn)	(Million L)	(Metric tn)	(Metric tn)	(Metric tn)	(tn)	(Million L)
A	1960	Goggin Drain near Magna, UT	–	153,000	215,000	110,000	381,000	–	–
	1961	Goggin Drain near Magna, UT	–	75,000	135,000	69,000	240,000	–	–
	1964	Goggin Drain near Magna, UT	44,000	46,000	61,000	31,000	109,000	77,000	46,000
	2013	Goggin Drain near Magna, UT	111,000	74,000	43,000	22,000	76,000	–	–
B	1960	Weber River near Plain City, UT	57,000	153,000	58,000	32,000	98,000	53,000	153,000
	1961	Weber River near Plain City, UT	33,000	75,000	34,000	19,000	56,000	34,000	75,000
	1964	Weber River near Plain City, UT	109,000	385,000	112,000	62,000	187,000	108,000	385,000
	2013	Weber River near Plain City, UT	34,000	92,000	47,000	26,000	79,000	–	–
C	1960	Bear River at Corinne, UT	–	–	–	–	–	–	–
	1961	Bear River at Corinne, UT	–	–	–	–	–	–	–
	1964	Bear River at Corinne, UT	451,000	1,155,000	777,000	380,000	1,420,000	697,000	1,155,000
	2013	Bear River at Corinne, UT	459,000	624,000	496,000	242,000	907,000	–	–
D	1960	Bear River Causeway	–	–	–	–	–	639,000	787,000
	1961	Bear River Causeway	–	–	–	–	–	527,000	555,000
	1964	Bear River Causeway	–	–	–	–	–	1,259,000	1,126,000
	2013	Bear River Causeway	123,000	743,000	6,749,000	1,343,000	20,802,000	–	–
E	1960	Farmington Bay Causeway	–	–	–	–	–	286,000	223,000
	1961	Farmington Bay Causeway	–	–	–	–	–	216,000	163,000
	1964	Farmington Bay Causeway	–	–	–	–	–	973,000	347,000
	2013	Farmington Bay Causeway	443,000	252,000	9,286,000	1,665,000	30,042,000	–	–

	Regressed WY	Mean daily WY	LOADEST WY2013 TDS load			Hahl, 1968 WY	Mean daily WY
	2013 TDS load	2013 Streamflow	Average	Low 95% CI	High 95% CI	1964 TDS load	1964 Streamflow
	(tn)	(acre-ft)	(tn)	(tn)	(tn)	(tn)	(acre-ft)
Sum A, B, D, E	711,000	1,161,000	16,125,000	3,057,000	50,999,000	2,417,000	1,904,000
Sum A, B, C, E	1,046,000	1,042,000	9,872,000	1,956,000	31,104,000	1,855,000	1,933,000

4.2. Multi-variate analysis for continuous TDS loads

Statistical estimation methods include adjusted maximum likelihood estimation (AMLE), maximum likelihood estimation (MLE), and least absolute deviation (LAD). Our models use the AMLE because they were normally distributed with uncensored data. Given a time series of discharge and constituent concentrations such as TDS, LOADEST develops a regression model for the load estimation. Explanatory variables within the regression model include functions of streamflow, decimal time, and other variables. These estimates may be a better predictor of inflow dissolved solids loading because they take into account lag time associated with surficial salt storage in runoff, seasonality, and dilution, and provide predictive confidence limits of the estimate uncertainty. Our individual model evaluation criteria, the AMLE regression statistics, and the bias diagnostics for each of the monitoring locations are provided in Table 2.

As described in Fig. 6, we used the linear regressions of TDS to discharge for the period of record to estimate the daily TDS load into GSL for water year 2013. We then used the LOADEST model to develop the daily TDS load into GSL over the entire period of record. The average daily TDS load estimated with LOADEST and encompassed by the 95% uncertainty bounds for water year 2013 is provided in Fig. 7. In addition, the calculated loads based on the previously described TDS versus discharge regression algorithm for water year 2013 and for the entire period of record are provided for comparative purposes. Observed TDS and estimated TDS (SC) sample values are also presented in Fig. 7.

Our results indicate that regressed TDS loads were consistent with LOADEST predicted TDS loads for locations with increased sampling frequency over the period of record (Fig. 7). The regressed TDS loads for the Weber River and Bear River near Corinne sites were within the 95% confidence intervals throughout the majority of water year 2013 and reproduced observed trends reasonably well. These locations along with the Goggin Drain location had a higher sampling frequency resulting in better agreement between methods. However, the regressed estimates for the Goggin Drain location indicated poor agreement with generally higher values after January 1, 2013. The discrepancy between the TDS load estimates as a function of discharge and the LOADEST multi-variate TDS load estimates is largely a function of the variability in time between discharge measurements as an explanatory variable and the resulting TDS load. Because LOADEST incorporates time and seasonality as predictor variables, the results suggest that there are time lags associated with terrestrial and in-stream storage of salt storage prior to delivery.

The LOADEST results for the Bear River Causeway and Farmington Bay Causeway monitoring locations showed much higher variability in TDS loading than the other locations. This result is in large part due to the decreased sampling frequency at these locations and the difficulty in obtaining accurate discharge and water quality measurements. For example, when a wind-based seiche forces flow reversals of more saline water into the bay, a period of time is required to flush the GSL derived salinity from the bay. When continuous measurements are not available, there is no sufficient proxy to estimate system recovery and samples may consist of a mixture of GSL-derived and bay-derived salinity contributions resulting in artificially elevated TDS load estimates. Therefore, it is difficult to ascertain whether a sample is consistent with wind-driven seiches or a product of the TDS load from the bay. However, based on the sampling frequency for water year 2013, we can begin to constrain the predicted TDS load into the GSL using LOADEST.

Fig. 7. Comparison of daily load estimations, the mean daily flux (black) and the 95% confidence interval (gray) are shown. The daily discharge regressed load estimation over the period of record (red dash) and over water year 2013 (blue dash) are also given. Calculated loads are based on the product of mean daily discharge and samples measured for TDS concentration or regressed from specific conductance.

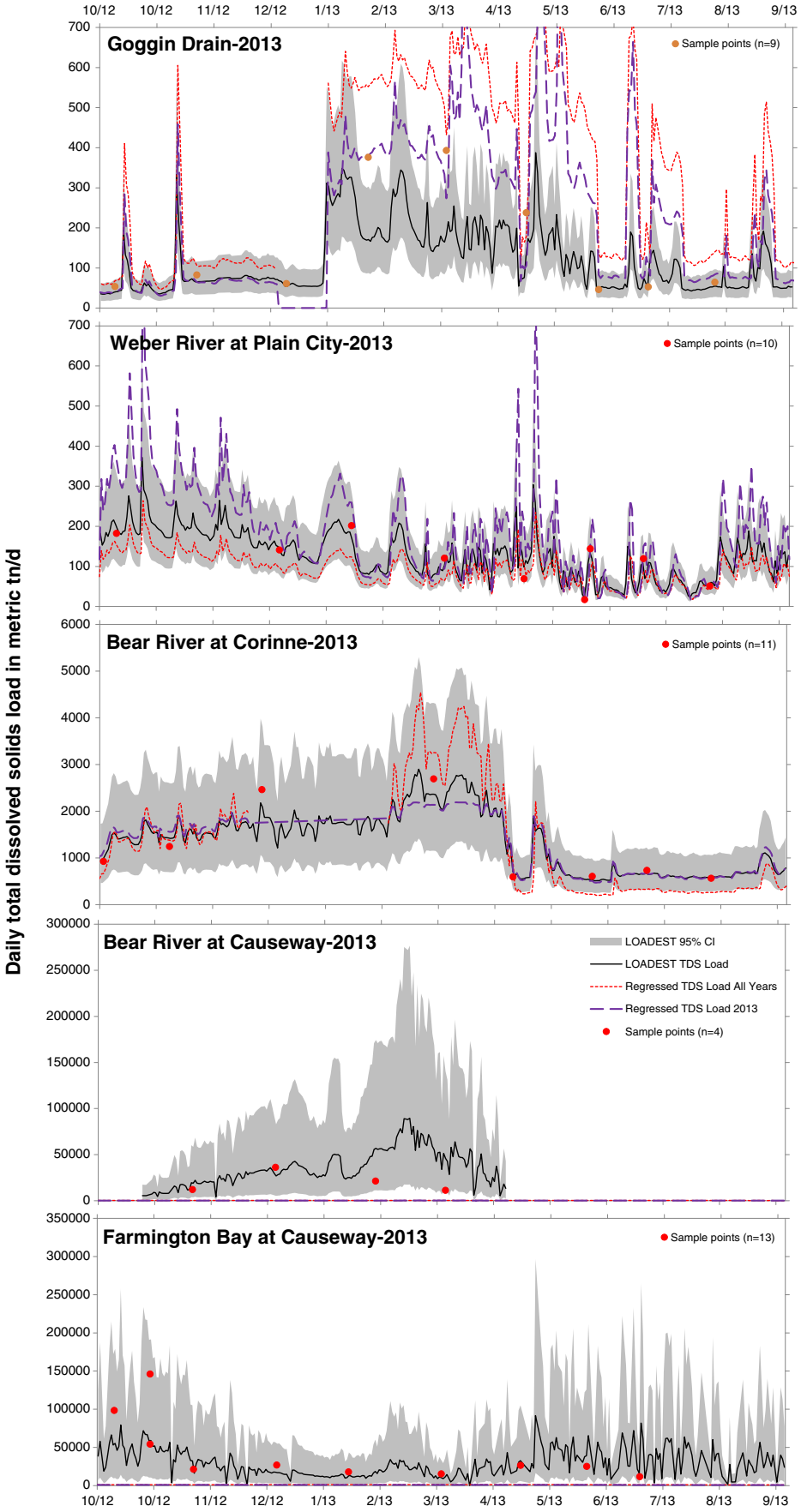
Daily total dissolved solids load in metric tn/d
10/12
10/12
11/12
12/13
1/13
2/13
3/13
4/13
5/13
6/13
7/13
8/13
9/13
Goggin Drain-2013
Sample points (n=9)
Weber River at Plain City-2013
Sample points (n=10)
Bear River at Corinne-2013
Sample points (n=11)
Bear River at Causeway-2013
LOADEST 95% CI
LOADEST TDS Load
Regressed TDS Load All Years
Regressed TDS Load 2013
Sample points (n=4)
Farmington Bay at Causeway-2013
Sample points (n=13)

5. Discussion and interpretation

5.1. Variability between regression based estimates and LOADEST

A key reason for the variability between regression based estimates and LOADEST estimates is that regression based estimates are strictly a function of TDS and discharge, while LOADEST estimates account for time variability. Based on our regressions, the average R^2 values for individual years at each monitoring location ranged between 0.17 and 0.61, indicating that there was significant uncertainty in the TDS estimates as a function of discharge. From SI 1, the R^2 of regressions for each of the years was 0.61 ± 0.29 for Goggin Drain, 0.38 ± 0.31 for the Weber River, 0.53 ± 0.37 for the Bear River at Corinne, 0.60 ± 0.32 for the Bear River at the Causeway, and 0.17 ± 0.18 for the Farmington Bay Causeway. What stands out is that the results from the Goggin Drain monitoring location had the highest coefficient of determination; however, the comparison with results estimated by LOADEST are not as robust as with the Weber River and the Bear River near Corinne. LOADEST point loads shown in Fig. 7 were estimated by calculating TDS from the previously described algorithm as a function of SC and multiplying by the discharge measured at that point in time. This differs considerably from Hahl's (1968) interpretation; our results were temporally variable versus his time and discharge weighted annual estimate. The regressions use the same model of TDS estimates as a function of instantaneous discharge but are subsequently aggregated for daily load estimates. Therefore, deviations are a function of how closely the point measurement accounts for the daily average.

The 95% confidence intervals with the LOADEST estimates indicate that for the Goggin Drain, Weber River at Plain City, and Bear River at Corinne monitoring locations, there is an average deviation of 48% below and 75% above the average load, respectively. However, for the Bear River and Farmington Bay Causeway locations, the average deviation about the mean load is 81% and 215%, respectively. While this indicates substantial uncertainty, it does provide boundaries for load estimates that can be minimized with better predictive capacity through additional samples distributed throughout the range of environmental conditions. When comparing the annual regressed load to LOADEST, we found that the regressed estimate with all data and with just 2013 at Goggin was 61% and 46% higher, respectively than the LOADEST estimate. Bear River Corinne was 8% and 7% lower, respectively. The Weber River was 39% lower and 29% higher, respectively. The Bear River Causeway and the Farmington Bay Causeway were 5300% and 2000% lower, respectively. This suggests that using annually based regressions are more consistent with the statistical estimates that incorporate more predictor variables, including time. It also shows the error introduced by estimating TDS loads solely based on discharge records.

5.2. Variability between WY 2013 and previous studies

We analyzed the estimated TDS load into GSL using regressions for the entire period of record and for individual years. In particular, we compared our regressions with those of water years 1960, 1961, 1964 and found that the Bear River and Farmington Bay Causeway samples were not included in previous estimates. We used the mean daily discharge at each location to calculate the annual TDS load based on our regressions of TDS as a function of discharge for each of the years. As Table 1 shows, our estimates were consistent with those of Hahl (1968) for the Weber River near Plain City, although the other monitoring locations showed much more deviation in annual TDS loads. For example, our annual linear interpolation regression of the Goggin Drain location in 1964 was 98% R^2 and we calculated nearly the same discharge as previously estimated. However, the deviation in total annual TDS load from the Goggin Drain is considerable. Therefore, while we cannot sufficiently reproduce the estimates of Hahl (1968) in every instance, we were able to quantify the expected load from the more robust estimates from LOADEST and quantify measurement uncertainty.

In the previous study, Hahl (1968) used the available measured data from each location for each of the three years of interest (1960, 1961, and 1964) to calculate the time (and possibly discharge) weighted average for each analyte (i.e.: discharge, TDS). He used the daily discharge sum to calculate the annual discharge. He then converted the TDS concentration units and calculated the product of discharge and TDS concentration to calculate the total TDS load. Our approach was to build a regression of TDS as a function of SC for more periods than TDS was sampled since there was a highly correlated TDS and SC relationship. We then regressed TDS to mean daily discharge to predict temporal variability, which is different than the average methodology that Hahl (1968) used. His results calculate a time weighted average for each year, although this approach does not incorporate event-based and seasonal variability unless they were adequately sampled. While our estimates varied from Hahl's (1968) results, they were generally within the uncertainty range and since the Hahl (1968) data were reported to the thousands, it suggests limited precision. Based on the accuracy of the regression and LOADEST for the different locations over different years relative to the only other analysis to our knowledge, our estimate of 2013 can be considered reasonable.

The variability in reproducing similar estimates may also be a function of inflow differences between the 1960, 1961, and 1964 data to that of 2013. Water years 1960, 1961, and 1964 were identified as low, low, and average water years, respectively (Hahl, 1968). The GSL stage differences between 1960, 1961, and 1964 relative to 2013 were 90.8%, 81.6%, and 78.9%, respectively, suggesting the 1960s had lower inflows to GSL, relative to average water years, and potentially higher TDS loads. While the approach of Hahl (1968) is reasonable, the difficulty is that the periods investigated had very low lake elevations after a decade of low lake levels which can be assumed to indicate less inflows. Hahl (1968) accounted for a substantial number of other inflows including near-lake seepage, groundwater discharge, WWTP effluent, and regression for near-shore processes. The near-shore estimates of evapotranspiration, precipitation, and groundwater discharge were elusive and more difficult to reproduce. Climatic conditions would also have varied the production of surficial salt stores and therefore, comparisons between years may not be reasonable due to increased climatic-based errors. Finally, road deicing has been shown to contribute to up to 25 times higher Na and Cl lake concentrations with distinct seasonality (Novotny et al., 2008). As population in the GSL watershed has increased, it is expected that road deicing and the associated environmental impacts has increased.

5.3. Quantification of uncertainty

By using LOADEST, we built upon previous studies (Hahl, 1968; Loving et al., 2000) with more robust sampling and by quantifying estimate uncertainty. We compared the upper 95% as a percentage difference from the mean for SC, TDS, period of record, and average number of days per measurement for each of the monitoring locations (Fig. 8).

Results indicate that the higher the number of samples (SC and TDS), the lower the 95% confidence interval difference from the mean or decreased uncertainty. In addition, the longer the period of record, the lower the uncertainty because the probability of the full range in environmental conditions is increased. However, the average number of days per measurement is not well correlated to decreased uncertainty as it is dependent on the range of conditions more than sampling interval. To bolster this analysis, we analyzed a dataset where discharge and SC were collected continuously throughout 2013. With the hypothesis that decreased measurement frequency leads to increased uncertainty. The dataset was the USGS 09180500 Colorado River near Cisco, UT streamgage monitoring location. While this monitoring location was outside the studied watershed, there was not a continuous dataset within the watershed and this location is representative to test the hypothesis. SC and discharge measurements were collected every 15 min at the Cisco location, and then we resampled the continuous data at

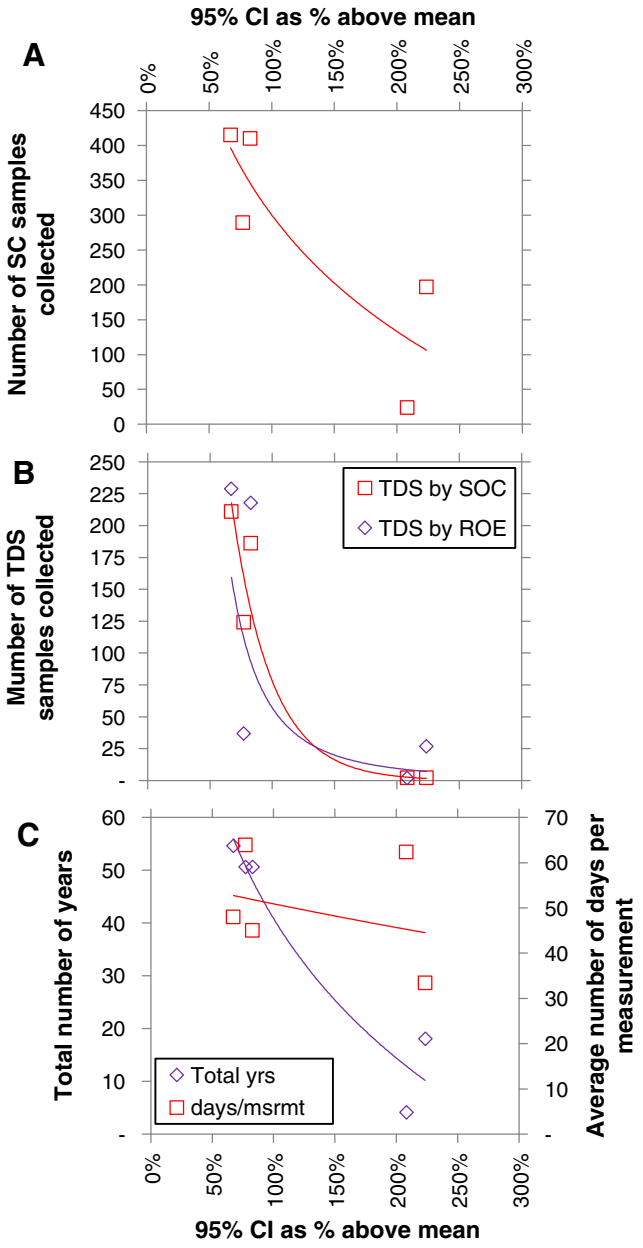

Fig. 8. Estimate of relative uncertainty as a function of the number of specific conductivity, total dissolved solids samples, the period of record, and the average number of days per sample.

bi-daily, daily, weekly, bi-monthly, and monthly intervals. We used LOADEST to quantify estimate uncertainty based on the resampling (Fig. 9).

Results indicate that sampling even twice per day can produce significant uncertainty at up to 15% variability about the mean. The daily sampling interval result is similar to bi-daily and weekly only a little bit more uncertain. This suggests that weekly monitoring is similar to bi-daily, if the monitoring effort is limited by financial or logistical concerns. However, bi-monthly is much more uncertain and monthly sampling did not accurately quantify the continuous TDS load at the Colorado River near Cisco site. When we investigated TDS as a function of discharge at Colorado River near Cisco, it is apparent that a single regression cannot quantify the variability in TDS as a function of discharge (Fig. 10).

During peak runoff when the TDS is lowest (red), there is a significant deviation from the remainder of the year. In addition, the obvious hysteretic effects limit the predictive power of intervals less than continuous for this monitoring location. This is important because landscape, terrestrial, and climatic processes all play a role in TDS export limiting the ability to regress solely based on discharge.

6. Summary and conclusions

In this study, we analyzed the total dissolved solids loading into the Great Salt Lake (GSL), the largest hypersaline lake in the Western Hemisphere, for water year 2013. We compared these estimates with those of previously sampled periods in the early 1960s. Further, we used the LOADEST statistical model to quantify the uncertainty in the observed loading estimates. Our estimates indicate that TDS loading to the GSL in water year 2013 was 16.1 million tons an uncertainty of 2.8 to 46.3 million metric tons, which is significantly different from previous operational estimates based on water year 1964 of 2.7 million metric tons. These dissolved solid load estimates are important because of the rich ecosystem diversity that the GSL supports as a part of the Western Hemisphere Shorebird Reserve Network. The GSL also supports productive brine shrimp aquaculture and mineral extraction industries, influenced by the transfer and movement of solutes into and within the lake. These features elucidate the need for accurate spatiotemporal assessment of dissolved solids loading into the GSL.

Our results indicated that dissolved solids loads throughout the north arm of the GSL were elevated relative to the south arm, which is not surprising due to the higher dissolved solids concentrations, minimal inflows, and greater volume. Temporally, both the north and south arm dissolved solids loads are correlated with lake elevation. However, the annual average dissolved solids load within the GSL in water year 2013 was estimated at 4.11 billion metric tons, consistent with previous estimations.

The relationship between TDS concentration and surface water discharge also showed considerable variability, particularly at the Causeway sampling locations from the Bear River and Farmington Bays. These monitoring locations to the GSL were found to be influenced by periodic wind-driven seiches that forced water from the GSL into each of the bays and were subsequently dissipated into the GSL. The TDS versus discharge relationship typically benefitted from annual regressions rather than the previously mentioned period of record analysis; however there were still considerable discrepancies between the annual dissolved solids loading in water year 2013 and the sampled periods in the early 1960s. Therefore, we utilized the LOADEST model to better estimate GSL inflow dissolved solids loading associated with lag times and the uncertainty in these estimates.

We found that sampling locations with increased sampling frequency were more consistent with the loads calculated from simple regression models and that the 95% confidence intervals were typically minimized. Because time is incorporated into the LOADEST models, discrepancies are expected to be largely a function of temporally lagged salt storage delivery to the GSL associated with terrestrial and in-stream processes. We also present the effect of increased uncertainty as a function of decreased sampling frequency both from the available data and from an additional dataset. We demonstrate that by resampling continuous measurements at a decreased frequency, the 95% confidence interval increases substantially. Our experiment showed that this is primarily a function of spring discharge runoff associated with streams in much of the arid west.

These results benefit current and future management activities throughout the GSL by quantitatively providing spatiotemporal estimates of dissolved solids loading into the GSL bounded by the 95% confidence interval. Previous estimates collected solely in the early 1960s and using a time-weighted annual average have shown to be significantly different from regression-based estimates. By incorporating temporally variable estimates and statistically derived uncertainty of these estimates, we have provided quantifiable variability in the annual estimates of dissolved solids loading into the GSL. Further, our results

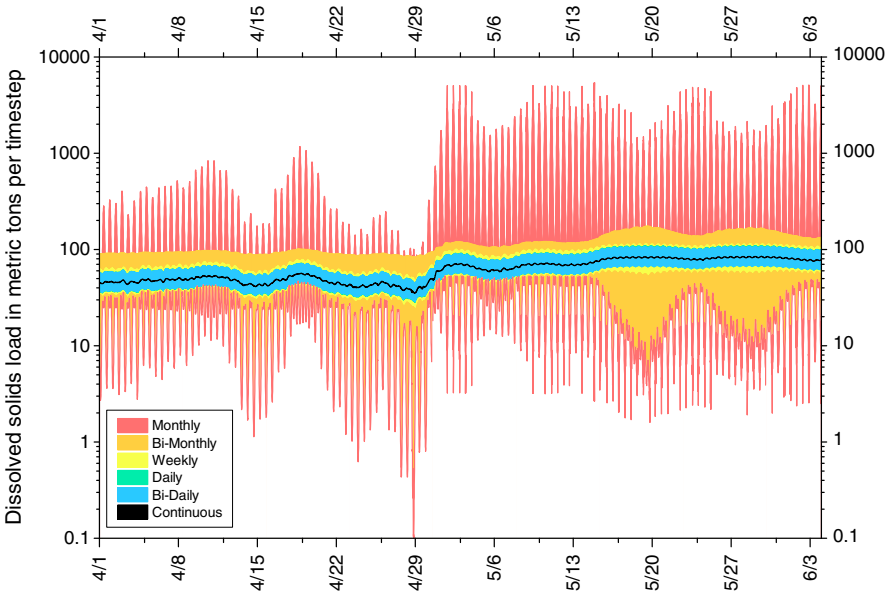

Fig. 9. Example of the range of uncertainty in TDS estimates calculated from the LOADEST model for April 1 through June 4, 2013 at the USGS streamgage location 09180500 Colorado River near Cisco, UT. Continuous measurements of discharge and TDS were used to resample at the different intervals with decreased fidelity.

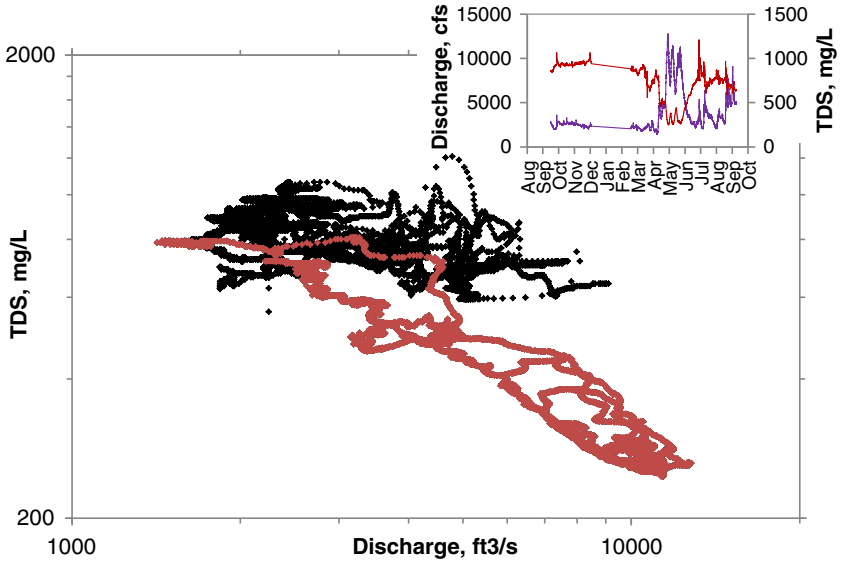

Fig. 10. Example of the continuous TDS concentration as a function of discharge for the USGS streamgage location 09180500 Colorado River near Cisco, UT. The points in red are those from peak flow spring runoff conditions of April 28 through July 11, 2013 as shown on inset. The inset figure describes the temporal variability in discharge (blue) and total dissolved solids concentration (red) throughout water year 2013.

support the need for increased monitoring of dissolved solids loading into the GSL by demonstrating the uncertainty associated with different levels of sampling frequency. Potentially 10% of the GSL dissolved salts could be contributed from inflows in less than a few decades and as little as 8 years. Therefore, a better understanding of salt contributions on this delicate ecosystem is warranted.

Supplementary data to this article can be found online at http://dx.doi.org/10.1016/j.scitotenv.2015.07.015.

Acknowledgments

We greatly appreciate the funding resources for this investigation allocated through the Utah Department of Natural Resources, Utah Division of Forestry, Fire and State Lands under grant number 1305448 and partial funding through the U.S. Geological Survey Cooperative Water Program. We also acknowledge the thorough and thoughtful reviews by David Naftz and two additional reviewers, that have significantly benefitted the manuscript.

References

Aherne, J., Larssen, T., Cosby, B.J., Dillon, P.J., 2006. Climate variability and forecasting surface water recovery from acidification: modelling drought-induced sulphate release from wetlands. Sci. Total Environ. 365, 186–199. http://dx.doi.org/10.1016/j.scitotenv.2006.02.041.

Akaike, H., 1973. Information theory and an extension of the maximum likelihood principle. 2nd International Symposium on Information Theory. Akadémiai Kiadó, Tsahkadsor, Armenia, pp. 267–281.

Akaike, H., 1974. A new look at the statistical model identification. IEEE Trans. Autom. Control AC-19, 716–723.

Aldrich, T.W., Paul, D.S., 2002. Avian ecology of Great Salt Lake. In: Gwynn, J.W. (Ed.), Great Salt Lake: An Overview of Change. Utah Department of Natural Resources and Utah Geological Survey Special Publication, Salt Lake City, UT, pp. 343–374.
Cohn, T.A., 1988. Adjusted maximum likelihood estimation of the moments of lognormal populations from type 1 censored samples, Open-File Report, U.S. Geological Survey, Open-File Report 88-350. Reston, VA , p. 34 http://pubs.er.usgs.gov/publication/ofr88350.
Cohn, T.A., 2005. Estimating contaminant loads in rivers: an application of adjusted maximum likelihood to type 1 censored data. Water Resour. Res. 41, W07003. http://dx.doi.org/10.1029/2004WR003833.
Cohn, T.A., Delong, L.L., Gilroy, E.J., Hirsch, R.M., Wells, D., 1989. Estimating constituent loads. Water Resour. Res. 25, 937–942. http://dx.doi.org/10.1029/WR025i005p00937.
Cohn, T.A., Caulder, D.L., Gilroy, E.J., Zynjuk, L.D., Summers, R.M., 1992. The validity of a simple log-linear model for estimating fluvial constituent loads: an empirical study involving nutrient loads entering Chesapeake Bay. Water Resour. Res. 28, 2353–2364. http://dx.doi.org/10.1029/92WR01008.
Colman, S.M., Kelts, K.R., Dinter, D.A., 2002. Depositional history and neotectonics in Great Salt Lake, Utah, from high-resolution seismic stratigraphy. Sediment. Geol. 148, 61–78.
Crawford, C.G., 1991. Estimation of suspended-sediment rating curves and mean suspended-sediment loads. J. Hydrol. 129, 331–348. http://dx.doi.org/10.1016/0022-1694(91)90057-O.
Dolan, D.M., Yui, A.K., Geist, R.D., 1981. Evaluation of river load estimation for methods for total phosphorus. J. Great Res. 7, 207–214. http://dx.doi.org/10.1016/S0380-1330(81)72047-1.
Elsdon, T.S., De Bruin, M.B.N.A., Diepen, N.J., Gillanders, B.M., 2009. Extensive drought negates human influence on nutrients and water quality in estuaries. Sci. Total Environ. 407, 3033–3043. http://dx.doi.org/10.1016/j.scitotenv.2009.01.012.
Ferguson, R.I., 1986. River loads underestimated by rating curves. Water Resour. Res. 22, 74–76. http://dx.doi.org/10.1029/WR022i001p00074.
Ferguson, R.I., 1987. Accuracy and precision of methods for estimating river loads. Earth Surf. Process. Landf. 12, 95–104. http://dx.doi.org/10.1002/esp.3290120111.
Fishman, M.J., 1993. Methods of Analysis by the U.S. Geological Survey National Water Quality Laboratory; Determination of Inorganic and Organic Constituents in Water and Fluvial Sediments.
Fishman, M.J., Friedman, L.C., 1989. Methods for Determination of Inorganic Substances in Water and Fluvial Sediments. U.S. Geological Survey, Alexandria, VA.
Guo, Y., Markus, M., Demissie, M., 2002. Uncertainty of nitrate-N load computations for agricultural watersheds. Water Resour. Res. 38. http://dx.doi.org/10.1029/2001WR001149 (3-1).
Hahl, D.C., 1968. Dissolved-Mineral Inflow to Great Salt Lake and chemical Characteristics of the Salt Lake Brine: Summary for Water Years 1960, 1961, 1964. Utah Geological and Mineralogical Survey Water-Resources Bulletin 10. UT, Salt Lake City, p. 33 p.
Hurvich, C.M., Tsai, C.-L., 1989. Regression and time series model selection in small samples. Biometrika 76, 297–307. http://dx.doi.org/10.1093/biomet/76.2.297.
Jones, B.F., Naftz, D.L., Spencer, R.J., Oviatt, C.G., 2008. Geochemical evolution of Great Salt Lake, Utah, USA. Aquat. Geochem. 15, 95–121.
Lenz, P., Browne, R., 1990. Ecology of Artemia. In: Browne, R.A., Sorgeloos, P., Trotman, C.N.T. (Eds.), Artemia Biology. CRC Press, Boca Raton, FL, pp. 237–254.
Loving, B.L., Waddell, K.M., Miller, C.W., 2000. Water and salt balance of Great Salt Lake, Utah, and simulation of water and salt movement through the causeway, 1987-1998. U.S. Geological Survey Water-Resources Investigations Report 00-4221 32 http://pubs.usgs.gov/wri/2000/4221/report.pdf.
Miller, D.M., 1991. Mesozoic and Cenozoic tectonic evolution of the northeastern Great Basin. In: Buffa, R.H., Conyer, A.R. (Eds.), Geology and Ore Deposits of the Great Basin. Geol Soc Nev, Reno Nevada, pp. 202–228.
Mohammed, I.N., Tarboton, D.G., 2011. On the interaction between bathymetry and climate in the system dynamics and preferred levels of the Great Salt Lake. Water Resour. Res. 47, W02525. http://dx.doi.org/10.1029/2010WR009561.
Mohammed, I.N., Tarboton, D.G., 2012. An examination of the sensitivity of the Great Salt Lake to changes in inputs. Water Resour. Res. 48. http://dx.doi.org/10.1029/2012WR011908.
Nash, J.E., Sutcliffe, J.V., 1970. River flow forecasting through conceptual models part 1 — a discussion of principles. J. Hydrol. 10, 282–290.
Novotny, E.V., Murphy, D., Stefan, H.G., 2008. Increase of urban lake salinity by road deicing salt. Sci. Total Environ. 406, 131–144. http://dx.doi.org/10.1016/j.scitotenv.2008.07.037.
Preston, S.D., Bierman, V.J., Silliman, S.E., 1989. An evaluation of methods for the estimation of tributary mass loads. Water Resour. Res. 25, 1379–1389. http://dx.doi.org/10.1029/WR025i006p01379.
Robertson, D.M., Roerish, E.D., 1999. Influences of various water quality sampling strategies on load estimates for small streams. Water Resour. Res. 35, 3747–3759. http://dx.doi.org/10.1029/1999WR900277.
Robertson, D.M., Saad, D.A., 2011. Nutrient inputs to the Laurentian Great Lakes by source and watershed estimated using SPARROW watershed models. J. Am. Water Resour. Assoc. 47, 1011–1033. http://dx.doi.org/10.1111/j.1752-1688.2011.00574.x.
Runkel, R.L., 2013. Revisions to LOADEST.
Runkel, R.L., Crawford, C.G., Cohn, T.A., 2004. Load Estimator (LOADEST) — A FORTRAN Program for Estimating Constituent Loads in Streams and Rivers.
Ryberg, K.R., Vecchia, A.V., 2012. waterData—An R Package for Retrieval, Analysis, and Anomaly Calculation of Daily Hydrologic Time Series Data, Version 1.0.
Shiklomanov, I.A., 1990. Global water resources. Nat. Resour. 26, 34–43.
Shope, C.L., Gerner, S.J., 2014. Assessment of Dissolved-Solids Loading to the Colorado River in the Paradox Basin between Dewey Bridge and Gypsum Canyon, Utah, (Salt Lake City, UT). U.S. Geological Survey Scientific Investigations Report 2014-5031. http://pubs.er.usgs.gov/publication/sir20145031.
Shope, C.L., Bartsch, S., Kim, K., Kim, B., Tenhunen, J., Peiffer, S., Park, J.-H., Ok, Y.S., Fleckenstein, J., Koellner, T., 2013. A weighted, multi-method approach for accurate basin-wide streamflow estimation in an ungauged watershed. J. Hydrol. 494, 72–82. http://dx.doi.org/10.1016/j.jhydrol.2013.04.035.
Stenback, G.A., Crumpton, W.G., Schilling, K.E., Helmers, M.J., 2011. Rating curve estimation of nutrient loads in Iowa Rivers. J. Hydrol. 396, 158–169. http://dx.doi.org/10.1016/j.jhydrol. 2010.11.006.
Tweed, S., Grace, M., Leblanc, M., Cartwright, I., Smithyman, D., 2011. The individual response of saline lakes to a severe drought. Sci. Total Environ. 409, 3919–3933. http://dx.doi.org/10.1016/j.scitotenv.2011.06.023.
U.S. Geological Survey, variously dated. National field manual for the collection of water-quality data, Techniques of Investigations, book 9. (Chapter A1–A9), available online at http://pubs.water.usgs.gov/twri9A. Individual chapters published in 1997, 2003, 2004, 2005, 2006, 2007, 2008, 2012, 2014.
Van Stappen, G., 2002. Zoogeography. In: Abatzopoulos, T.J., Beardmore, J.A., Clegg, J.S., Sorgeloos, P. (Eds.), Artemia: Basic and Applied Biology. Kluwer Academic Publishers, Dordrecht, pp. 171–224.
Waddell, K.M., Gerner, S.J., Thiros, S.A., Giddings, E.M., Baskin, R.L., Cederberg, J.R., Albano, C.M., 2004. Water Quality in the Great Salt Lake Basins Utah, Idaho, and Wyoming, 1998–2001. U.S. Geological Survey Circular 1236 Salt Lake City, UT. http://pubs.usgs.gov/circ/2004/1236/.
Wilde, F.D., Radtke, D.B., Gibs, J., Iwatsubo, R.T., 1999. Collection of Water Samples.